IOP Conf. Series: Journal of Physics: Conf. Series **1015** (2018) 032001 doi:10.1088/1742-6596/1015/3/032001

Investigation of hydrodynamic characteristics of laminar flow condition around sphere using PIV system

A H Abed[1, 2], S E Shcheklein[1]

[1] Ural Federal University named after the first President of Russia B. N. Yeltsin
19 Mira St., Yekaterinburg 620002, Russia
[2] University of Technology, Iraq

E-mail: akraaam82@yahoo.com

Abstract. This paper aims to determine the hydrodynamic characteristics of flow around the sphere in unsteady state condition. An experimental test-rig was designed and constructed for this purpose with the application of an adjusted laser optics system. It is based on the technology of pulsed particle visualization of micro tracers in the cross section per unit time interval. Visualization with Particle Image Velocimetry (PIV-system) is used to study the properties of the flow such as its structure. The PIV-system is the most accepted technique allowed one to measure the instantaneous velocity distribution in fluid applications. In this experimental study, o-ring is used to simulate turbulence on the sphere surface and creates very high-level fluctuations, which creates the flow undergoing a laminar-to-turbulent transition. This transition leads to a delay of the separation point of flow from the sphere surface causing a significant reduction in the drag coefficient, reaching 45%. New results obtained can be useful in the development of numerical validation as well as in design processes.

1. Introduction

Investigation of flow hydrodynamic characteristics around a sphere in a uniform flow such as vortex shedding mechanisms, velocity field, pressure and drag coefficients is not only necessary in a practical field such as nuclear, chemical and energy fields, but it has also a good benchmark to predict the flow characteristics for designing purposes [1]. There are numerous numerical and experimental studies concentrated on flow characteristics and flow control to reduce the drag coefficients, using a sphere with dimples, roughened, vented spheres and other control methods [2]. In the early studies [3-7], the flow characteristics around a smooth sphere located in a uniform flow and further investigations cited therein were undertaken. Nakamura I [8] performed an experimental investigation of the wake behind a sphere using dyed water for visualization in the low Reynolds number range. According to the study, the vortex shedding behind a sphere was stable and axisymmetric in the range of Reynolds number (Re=7-10) and continued to preserve its steady state for Reynolds number up to 190. In the previous studies of the flow past a sphere, Zhao et al. [9] studied the vortex shedding, the drag coefficient and the flow structure of a sphere in the proximity of a flat plate using direct numerical simulation. The entire domain was presented as [48.85D*4.7D*3.5D] with different sphere center locations of 5.25D, 5.45D, respectively. The wake characteristics show an asymmetric structure with a separation angle [Θ= 89.5°] and a recirculation region with the length of 2.78D. In case when the sphere is smooth and the flow is in parallel layers (laminar regime), the fluid flow downstream separates from the surface of

the sphere in the form of vortices. This phenomenon is called flow-separation, causing a viscous wake behind the sphere and leads to increasing the drag force [10]. The roughness and dimples on the surface of a sphere act as turbulators, creating turbulence next to the sphere surface, which reduces the drag force to about (30-50%) compared with a smooth one [11]. Numerical and experimental investigations have been performed by Bogdanovic Jovanovic J et al. [12] to analyze the fluid flow characteristics around a sphere with dimples using Laser-Doppler-Anemometry (LDA). The investigation results indicate that the length of the re-circulation zone is reduced from 1.4 to 0.815 and the drag is reduced to about 30% for the wide range of Re due to a laminar-to-turbulent transition in the boundary layer. This transition leads to a delay of the separation point of flow from the sphere surface causing an essential reduction in the drag force. Alam F et al. [13] experimentally investigated the effect of different dimple shapes, depths and sizes on the aerodynamic behavior of the golf ball. The results show significant variation in so far as drag coefficient varies from 25 to 50% using different dimple shapes such as Circular, Hexagonal, Circular within Circular and Circular shallow. Applied flow control methods create a narrower wake region and shorter recirculation which, in turn, results in lower loading effects, drag and lift coefficients [14]. The flow structures around a sphere in the open water channel were experimentally investigated using particle image velocimetry (PIV) by Ozgoren M et al. [14]. Vented, roughened and smooth spheres with passive control are used to examine the effects of flow control methods on the sphere wake for Reynolds number (Re = 5000). They found that the reverse flow region in the wake is significantly reduced and flow separation around the sphere is delayed. In the present study, the drag coefficient, the flow pattern and velocity distribution around a sphere were experimentally studied using the particle image velocimetry (PIV) technique. All experiments were performed in a laminar flow regime with a range of Reynolds number (25-200) based on the free stream velocity. The sphere was placed in the flow of water stream and was sustained by stainless steel wires, which span across the plexiglas channel. To reduce the amount of the drag coefficient of a sphere, a passive method was tested successfully using o-ring.

2. The experimental Set-up and methods of results treatment

2.1. System description

An experimental test-rig was designed and constructed to represent a closed loop water system in the department of nuclear power plants and renewable energy sources at Ural Federal University, Russia. A schematic layout of the experimental set-up is shown in figure 1. To implement this experimental study, the test section is made from a 3 mm thick transparent plexiglas channel, which had a 50 mm diameter and a total length of 1100 mm. The cylindrical tank has a diameter of 800 mm and a length of 940 mm. To reduce the velocity disturbance, generated when the water is pumped, a non-pulsating metering pump (Grundfos Pump) is used for the present experiment. The sphere with a diameter of 24 mm was made of plexiglass placed in the flow of water stream and it is sustained by stainless steel wires which span across the plexiglass channel. The drag force can be measured by drag measuring devices also called drag balances using flexible beams fitted with strain gages to measure the drag force electronically. In this study, drag force is measured directly by attaching the sphere to a calibrated spring and measuring the displacement in the flow direction. The solution of equation (3) gives a drag force for any displacement vector (x). To reduce the drag coefficient, a turbulence insert is used in the form of o-ring made from rubber material with an outer diameter of 43.5 mm located at the front side of the sphere with a 16 mm inner diameter as shown in figure 2a. A flow meter type (Ty 4213) with an accuracy of (±0.3%) is used to measure the water volumetric flow rate. All sensors, pump and flow meter were connected to the data acquisition system with an accuracy of (±0.04%). Quantitative measurements of fluid velocity maps around a sphere have been carried out using Particle Image Velocimetry. The PIV system consists of five main parts which are:

- Digital cameras with resolution of up to 16 Mpix.
- Pulsed laser with light-sheet optics.

- Synchronizing device.
- Actual Flow software.
- Seeding particles for liquid and gas flows.

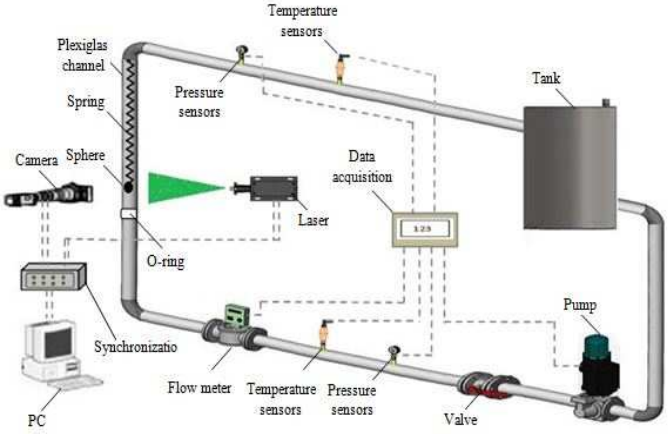

Figure 1. A schematic diagram of the experimental test-rig and the PIV method.

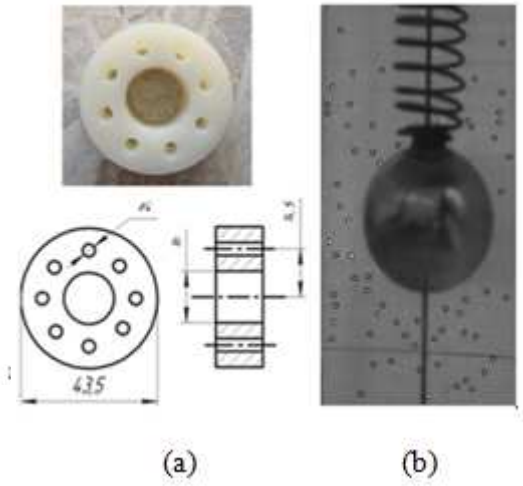

Figure 2. (a) Turbulence insert in the form of o-ring; (b) sphere with micro particles (trackers)

2.2. PIV system

The principle of measuring instantaneous velocity of the flow in a given cross section is based on the records of a shift of promiscuity particles in the cross section per unit time interval [15]. In this experimental investigation, POLIS measurement systems were used to study the hydrodynamic flow around a sphere in the low Reynolds number range from 25 to 200 based on the free stream velocity. Particle Image Velocimetry (PIV) is used to measure instantaneous flow velocity, flow pattern and velocity distribution around a sphere. PIV makes it possible to measure instantaneous velocity distributions in two and three component vector fields in a cross-section of a flow. In the flow of water, micro-particles (trackers) as shown in figure 2b are added and illuminated by a pulsed laser with light-sheet optics which is designed to handle a high power beam up to 380 mJ with beam diameter 150 mm. The method depends on the fact that small particles introduced in a water flow would move with the local water velocity and not respond to the buoyancy forces, see equation (5). Recording of the reflected optical laser pulses was done by the cross-correlation velocity digital camera, which is designed to make it possible to calculate the particle displacements during a time interval. Also, the PIV system contains an imaging system synchronized with the pulse laser and computer software for calculating the cross-correlation function between the images pairs.

3. Data processing

The purpose of the current study is to determine the drag coefficient for the sphere with and without passive control in the form of o-ring using Particle Image Velocimetry (PIV) technique. The parameters of interest are Reynolds number (Re) and drag coefficient (C_d). The Re is given by [11]:

$$Re = U \times D/\nu \,, \tag{1}$$

in which ν, D are fluid kinematics viscosity and a diameter of the sphere, and U is the mean fluid velocity.

Drag coefficient C_d is defined as [16]:

$$C_d = \frac{2\,(F_D - F_w)}{\rho\, U^2\, A} \tag{2}$$

where F_D represents the drag force determined by equation (3):

$$F_D = K_s \times X \tag{3}$$

and

$$F_w = w_s \times g. \tag{4}$$

The working fluid was seeded with tracer particles. The ability of tracer particles to follow up working fluid was measured using Stokes number. S_k is defined according equation (5), [17]:

$$S_k = \frac{t_p\, U}{d_c} \tag{5}$$

where t_p represents the response time of the particle determined by equation (6):

$$t_p = \frac{\rho_d\, d_d^2}{18\,\mu_{wf}}. \tag{6}$$

In the PIV system, the statistical velocity is calculated by the following equation [17]:

$$\bar{x} = \frac{1}{N}\sum_{i=0}^{N} x_i. \tag{7}$$

Here N is the number of valid measurements x_i

4. Experimental results and discussion

The experimental results of hydrodynamic characteristics around a smooth sphere with and without o-ring effects are presented. The results of the drag coefficient are compared with the past studies as shown in figure 3, which show the variation of drag coefficient versus Reynolds number with 8.4%. In figure 3, the C_d shows a decreasing trend with the increase in Reynolds number. The drag coefficient continues to decrease with increasing Reynolds number, which does not necessarily denote a decrease in drag force. The drag force is proportionate to the square of the velocity and the increase in velocity at higher Reynolds number is generally more than offsets in the decrease of the drag coefficient as shown in equation (2).

The drag coefficient for a smooth sphere is higher in laminar than in turbulent flow and in general is caused by two various effects (friction and pressure), which are usually difficult to determine separately [11, 19]. In the present study, o-ring as a passive flow control is used to simulate disturbance on the sphere surface to create very high-level fluctuations and the flow undergoes laminar-to-turbulent transition. This transition leads to a delay of the separation point of flow from the sphere surface causing a significant reduction in the drag coefficient, reaching 45% as shown in figure 4.

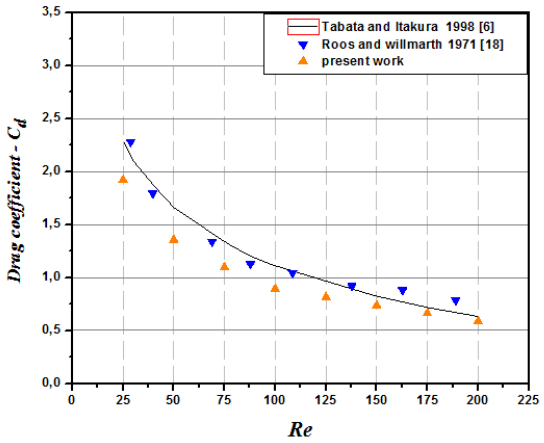

Figure 3. Variation of drag coefficient with Reynolds number for smooth sphere

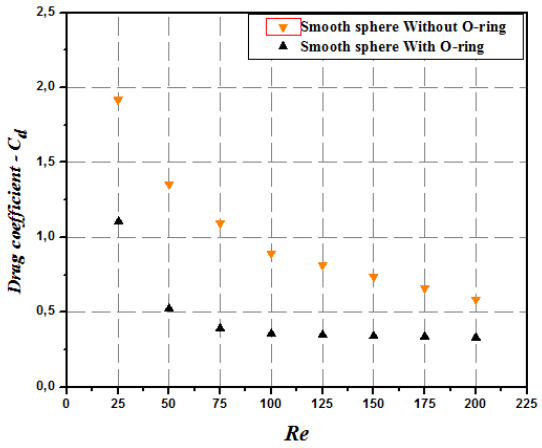

Figure 4. Variation of drag coefficient with Reynolds number for smooth sphere with and without o-ring for smooth sphere

Particle Image Velocimetry (PIV) measurement set POLIS was developed in the Institute of Thermo-physics SB RAS Novosibirsk - Russia used to measure the velocity felid around a sphere [20]. The velocity distribution was determined based on the statistical correlation function as shown in equation (7), which relates the number of valid measurements (numbers of an image captured). After image processing, in addition to 60 images, using the application program, the pictures shown in figure 5 are obtained. The present velocity field flow illustrates the velocity distribution around a sphere (figure 5b) and after o-ring (figure 5a). When scrutinizing figures, one can observe that the flow velocity after o-ring significantly increased and that leads to a retard of the separation point of flow from the sphere surface causing a significant reduction in the drag coefficient. The displacement with the correlation function, which relates the pixel intensity with particle distance, is applied to the entire image and the output is shown in figure 6.

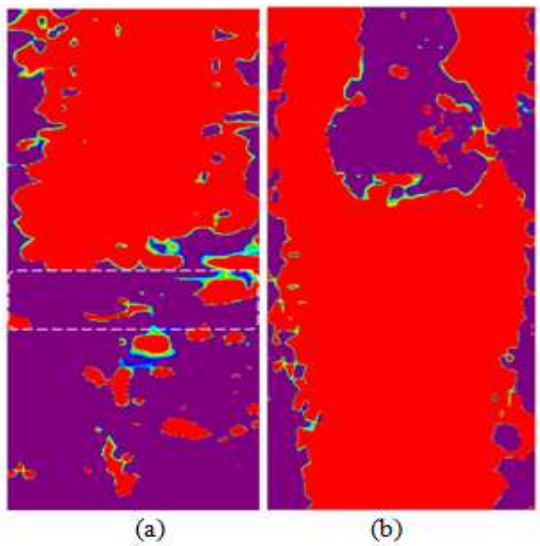

Figure 5. Fluid flow visualization: (a) mean velocity distributions before and after o-ring; (b) mean velocity distributions around a sphere

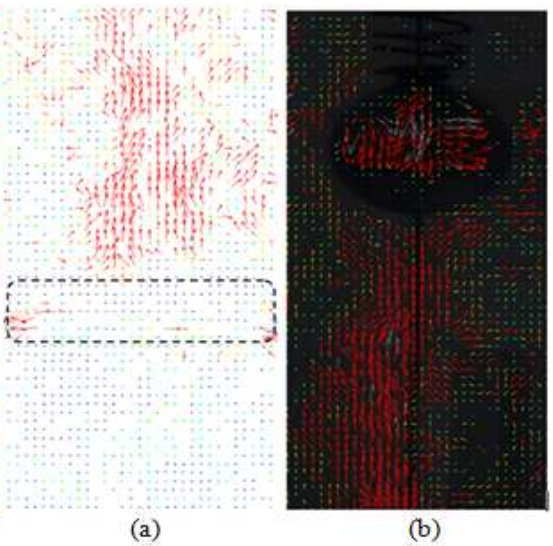

Figure 6. (a) Velocity vector after and before o-ring; (b) velocity vector around a sphere

5. Conclusions

In this paper, an experimental test-rig was designed and a Particle Image Velocimetry (PIV) measurement based on the pulsed imaging technology of micro-particles (trackers) was used to get information on non-stationary characteristics of hydrodynamic flow around the sphere. O-ring as a passive flow control used to simulate disturbance on the sphere surface, which allowed one to reduce the drag coefficient of the sphere in a closed water system is around 45% within the range of Reynolds number based on the free stream velocity. The experimental results were showing a good agreement with those obtained by other authors.

References

[1] Achenbach E 1974 *J. Fluid Mech.* **62(2)** 209-221
[2] Li J, Tsubokura M and Tsunoda M 2015 *Flow Turbul. Combust* **(95)** 415
[3] Achenbach E 1974 *J. Fluid Mech.* **65(1)** 113-125
[4] Taneda S 1978 *J. Fluid Mech.* **85(1)** 187-192
[5] Wu J S and Faeth G M 1993 *AIAA J.* **31(8)** 1448-1455.
[6] Tabata M and Itakura K 1998 *Int. J. Comput. Fluid D.* **9** 303-311
[7] Leweke T, Provansal M, Ormieres D and Lebescond R 1999 *Phys. Fluids* **11(9)** 12
[8] Nakamura I 1976 *Phys. Fluids* **19(1)** 5-8
[9] Zhao H, Liu X, Li D, Wei A, Luo K and Fan Jia 2016 *Int. J. Multiphas Flow* **79** 88-106
[10] Schlichting H 1968 *Boundary Layer Theory* (New York: Mc Graw-Hill)
[11] Cengel Y A and Cimbala J M 2013 *Fluid Mechanics Fundamentals and Applications* (New York: Mc Graw-Hill)
[12] Bogdanovic Jovanovic J, Stamenkovic Z, KOCIC M 2012 *thermal science* **16(4)** 1013-1026
[13] Alam F, Steiner T, Chowdhury H, Moria H, Khan I, Aldawi F, Subic A 2011 *5th Asia-Pacific Congress on Sports Technology APCST* (*Procedia Engineering* vol 13) ed Subic A, Fuss F K, Alam F and Clifton P (Melbourne: Elsevier) 226–231
[14] Ozgoren M, Dogan S, Okbaz A, Aksoy M H, Sahin B and Akilli H 2013 *EFM12* (*EPJ Web of Conferences* vol **45**) ed Dancova P and Novonty P (Hradec Kralove: EDP Sciences) 126-135
[15] Scarano F 2008 *Overwiew of PIV in supersonic flows Particle Image Velocimetry* (Berlin: Springer)
[16] Son K, Choi J, Jeon W and Choi H 2011 *J. Fluid Mech.* **672** 411- 427
[17] Raffel M and Willert C E 2007 *Particle Image Velocimetry-A Practical Guide* (Berlin: Springer)
[18] Roos F W and Willmarth W W 1971 *AIAA J.* **9(2)** 285-291
[19] Jang Y I and Lee S J 2008 *Exp. Fluids* **44(6)** 905-914
[20] Alekseenko S V, Bilsky A V and Markovich D M 2004 *Instruments and Experimental Techniques* **47(5)** 703-710